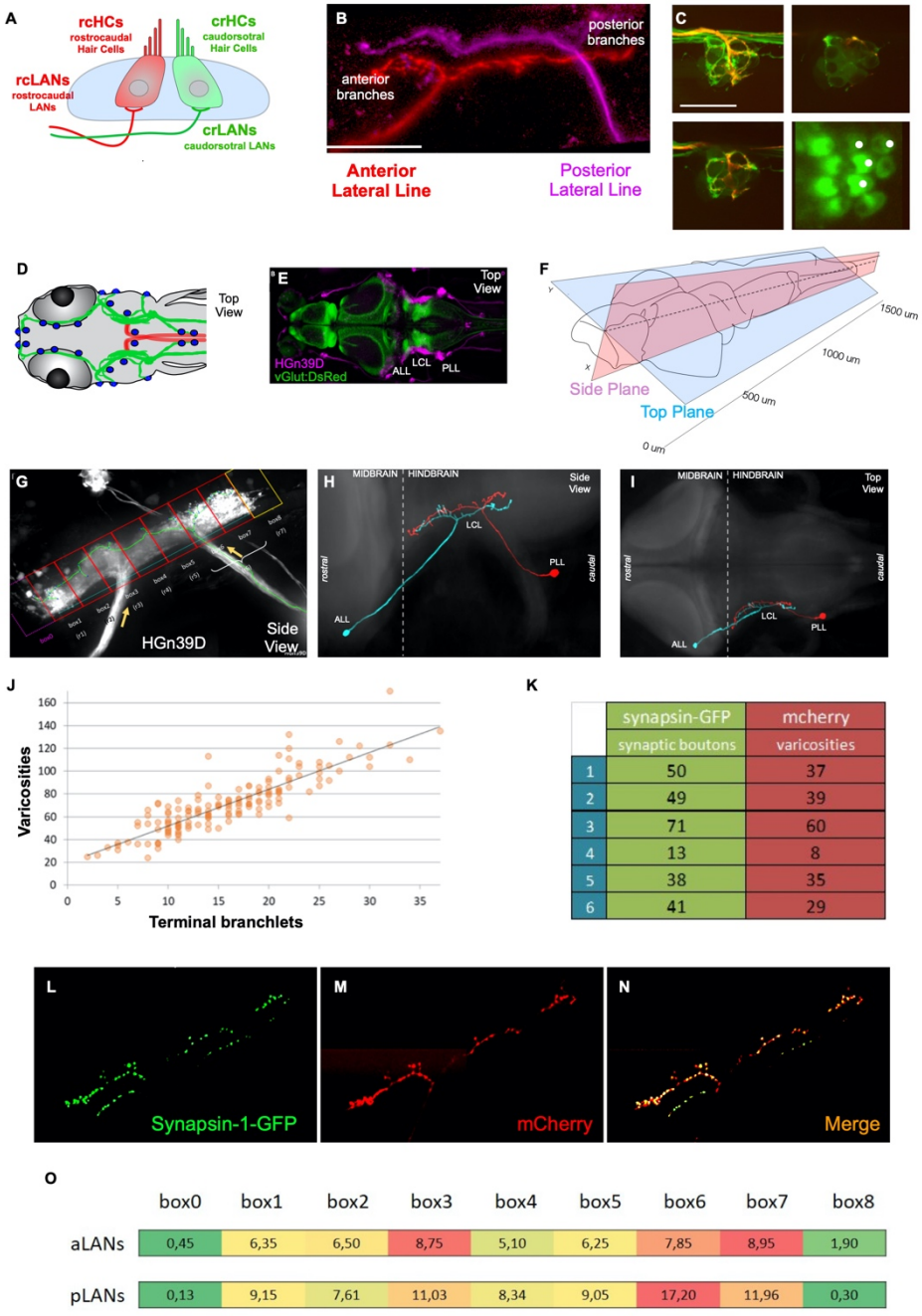

	synapsin-GFP synaptic boutons	mcherry varicosities
1	50	37
2	49	39
3	71	60
4	13	8
5	38	35
6	41	29

	box0	box1	box2	box3	box4	box5	box6	box7	box8
aLANs	0,45	6,35	6,50	8,75	5,10	6,25	7,85	8,95	1,90
pLANs	0,13	9,15	7,61	11,03	8,34	9,05	17,20	11,96	0,30

Figure S1. Lateral-line structure. Related to Figure 1. (**A**) Side view of a neuromast showing planar polarization of hair cells: rostrocaudal-oriented (rcHCs in red) and caudorostral-oriented (crHCs in green). rc-tuned and cr-tuned LANs are also depicted. (**B**) Confocal image of a larval zebrafish hindbrain highlighting the gross somatotopic organization of aLANs and pLANs central projections. A neuromast of the anterior lateral line (ALL) and one of the PLL were injected,

respectively, with red and magenta dextrans, which are transported to the brain by the corresponding LANs. The anterior and posterior branches of LAN central projections are indicated. (**C**) Maximal projection of a confocal series of a horizontal neuromast innervated by a singly-labeled LAN (red) and the entire LAN population (green). Individual optical sections reveal the peripheral arborization of the neuron at the basal and medial domains. The apical domain shows the planar polarization of hair cells, and white dots indicate the hair cells innervated by the marked neuron. (**D**) Scheme of the top view of the lateral-line system in the head of a zebrafish larva. LANs are shown in green. For reference, the reticulospinal Mauthner cells and their axons are in red and the neuromasts are represented as blue circles. (**E**) Top view of the maximal projection of the head of zebrafish larva in the double transgenic line *Tg[HGn39D ; vGlut:DsRed]* (respectively, magenta and green). The posterior (PLL) and anterior (ALL) lateralis ganglia and the lateralis central lintel (LCL) are indicated on the left hemisphere of the brain. (**F**) Scheme indicating the two orthogonal visualization planes with coordinates and indicative distances along the horizontal plane (side plane in pink and top plane in light blue). (**G**) Scheme of the “Box Method” showing the grid of 9 identical boxes. Below each box the rhombomere that approximately corresponds to the box is indicated. Yellow arrows indicate the points of entry of the axons of the ALL and PLL (respectively, approximately in rhombomeres 3 and 6). A single skeletonized pLAN (green) is superimposed to the transgenic line HGn39D (gray). (**H-I**) Volume-filled skeletons of one aLAN (cyan) and one pLAN (red) morphed on a reference brain (gray). (H) Side view and (I) top view. Both LANs project their central axons towards the LCL in the hindbrain. (**J**) Scatter diagram of terminal branches against varicosities, revealing a linear correlation between these parameters. (**K**) Table with the quantification of the number of varicosities and secondary branches in Synapsin-1-labeled LANs (green) and mCherry-labeled LANs (red) (N = 6). (**L-N**) Side views of the maximal projection of a pLAN co-expressing the presynaptic marker Sill:Synapsin-1-GFP (green in C) and Sill:mCherry (red in D). (E) shows the merging of both fluorophores. (**O**) Distribution of varicosities along the central arbor is similar between aLANs (above) and pLANs (below). aLANs show two peaks of high content of varicosities in box 3 and boxes 6-7 respectively. pLANs show one peak in boxes 6-7 and one less pronounced in box 3. Boxes are colored in a green-to-red scale from less to more varicosities. (**P**) Distribution of varicosities in

Ter_pLANs showing that Ter_rcpLANs (blue) have more varicosities than Ter_crpLANs (red). The difference in the number of varicosities is significant in box 1, 5 and 7 (p-values, respectively: 0.00508, 0.00666 and 0.00103; α = 0.01).

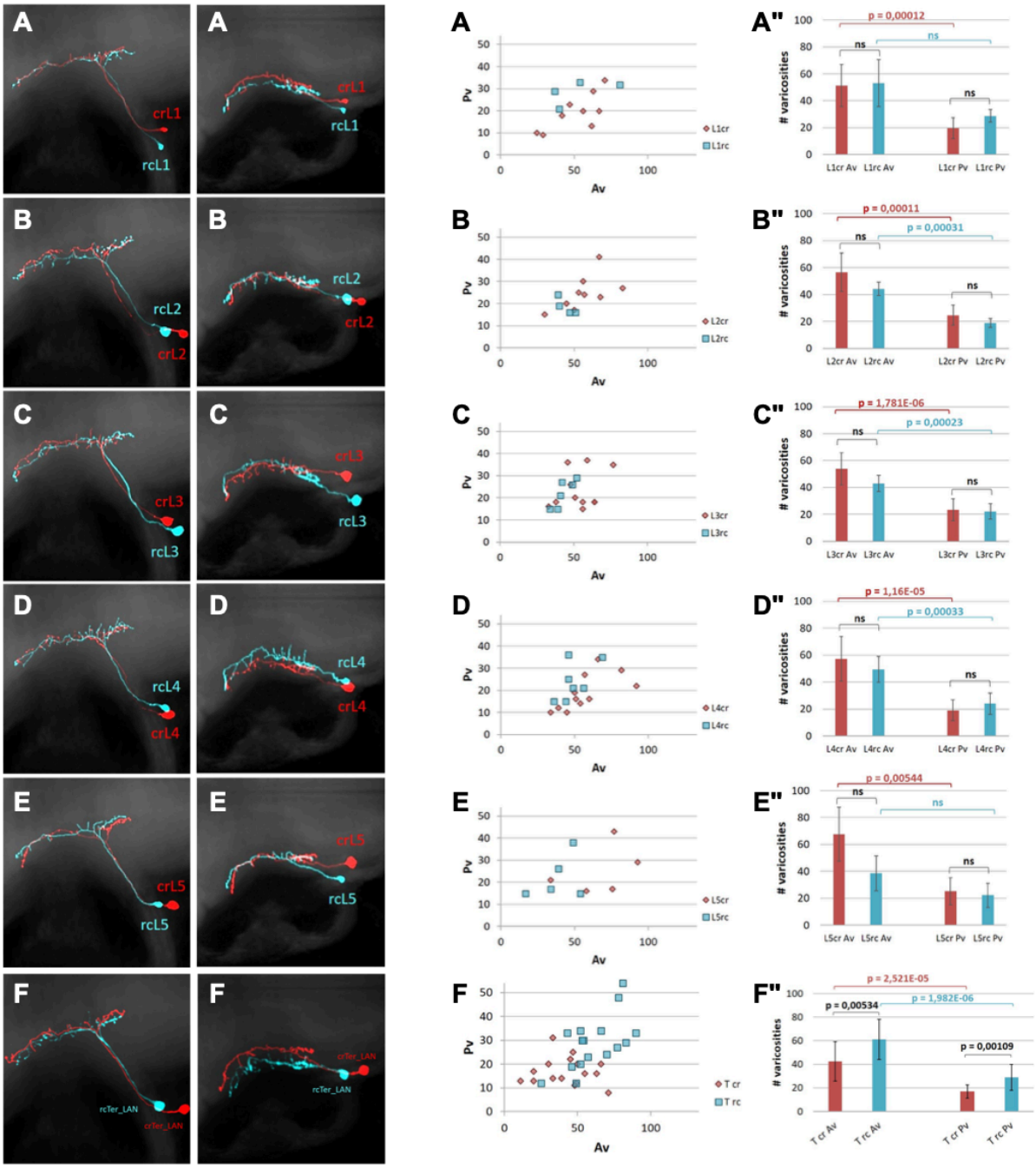

Figure S2. Anatomical characterization of lateralis afferent neurons. Related to Figure 2. (**A-E**) Side view of pairs of volume-filled skeletons of troncal LANs morphed onto a reference brain. They represent one L1-L5_crpLAN (red) and one L1-L5_rcpLAN (blue) clustered in separated groups from L1 to L5. (**A'-E'**) Top view

of the skeletons of (A-E). (**A‘‘-E‘‘**) crpLANs (red) and rcpLANs (blue) of the trunk of the fish (L1-L5) don not constitute clearly distinguishable morphological classes with respect to the number of AVs and PVs. (**A‘‘‘-E‘‘‘**) Bar graphs comparing the number of AVs (left) and PVs (right) between separated groups of L1-L5_crpLANs (red) and L1-L5_rcpLANs (cyan) show no significant differences (ns; $\alpha = 0.01$). (**F**) Side view of pairs of volume-filled skeletons of Terminal LANs morphed onto a reference brain. crTerLANs (red) and rcTerLANs (blue) can statistically be discriminated, albeit marginally, by the number of AVs and PVs.

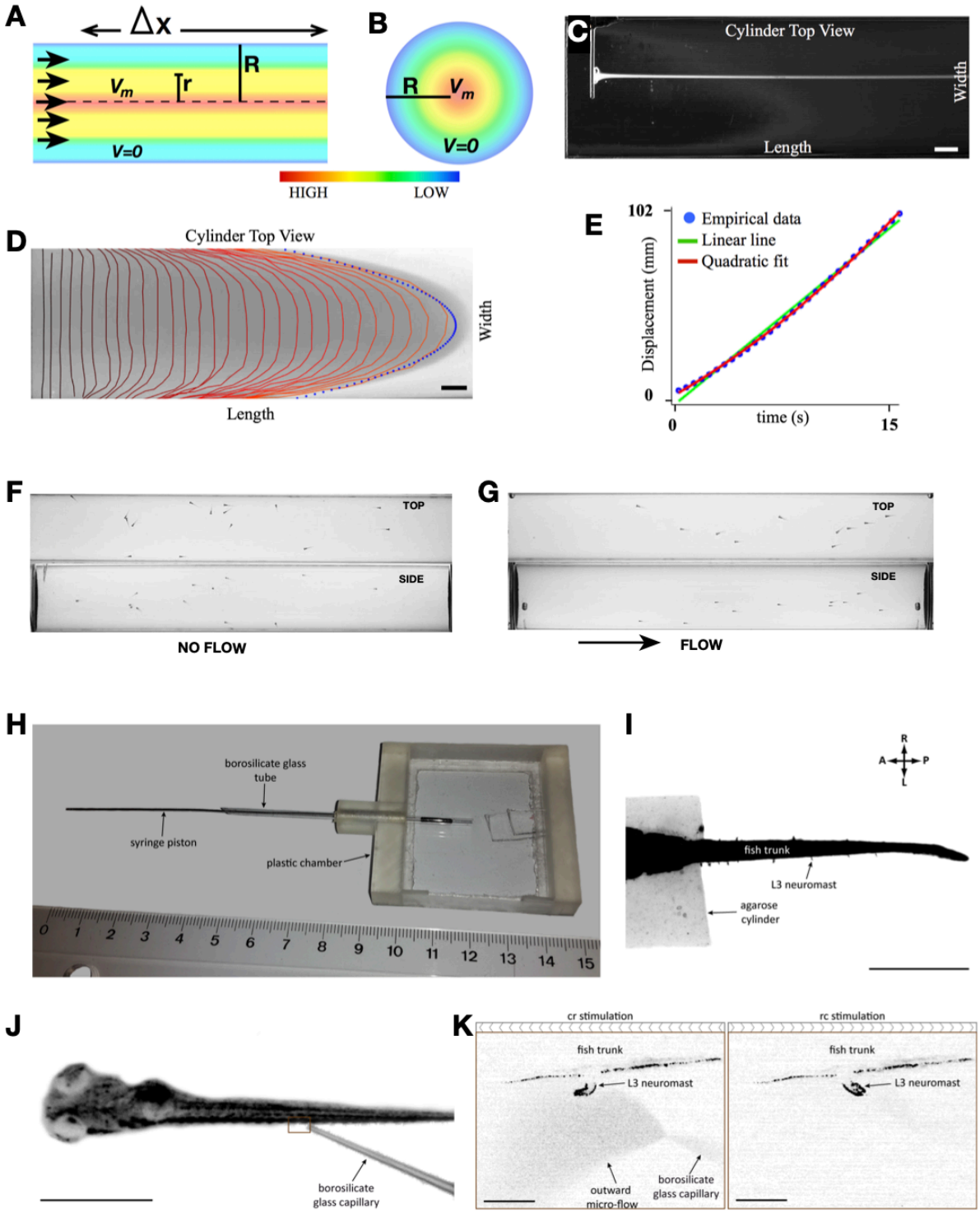

Figure S3. Experimental set-up for activity of lateralis neurons. Related to Figure 3 and 4. (**A-B**) Representation of a column of water moving at a constant velocity within a seamless cylinder, which generates an isosymmetric velocity gradient across the width of the cylinder. The rainbow- colored bar below the drawing describes the velocity gradient from high (red) to low (blue). Water flow is high in the center and low toward the periphery, being zero within the boundary layer between the water and the pipe's surface. (A) depicts a longitudinal and (B) a

transversal view of the cylinder. (**C**) Kymographs of the empirical test of water flow inside the rheotactic rig. A water-soluble dye (methylene blue) was delivered into the water through the tip of a syringe needle and videotaped. The straight line shows laminar flow at the center of the cylinder. (**D**) Kymographs of the empirical test of water flow inside the rheotactic rig. Here, the extreme of the cylinder closest to origin of the flow was filled with methylene blue and the displacement of the dye-front was videotaped and delineated in red at each time point. The flow velocity profile across the cylinder width is flat at the beginning of the movement and forms a parable when at full development, indicating laminar flow. (**E**) Plot of dye displacement (blue) at the center of the cylinder, fitting a linear increase (red). The slope of the fitted line is 6.8 mm/s while the plunger was moving at 5 mm/s. (**H**) Photograph of the mounting chamber. (**I**) An image of the trunk of a 7dpf larval zebrafish mounted in the chamber. The cupulæ of the neuromasts were labelled with fluorescent microspheres; red filter and green excitation light was used. (**J**) An image acquired by the camera of the two-photon setup showing the position of the electrode used for stimulation. Here and in (I), scale bars denote 1 mm. The area shown in (J) is outlined by an orange box. (**K**) Two-photon images of the L3 neuromast inclinations resulted from inward and outward microflow caused by stimulation, showing also the electrode tip filled with rhodamine solution and the outward flow during caudorostral stimulation. The stimulation electrode is not seen during rostrocaudal stimulation because negative pressure in the electrode results in filling it with non-fluorescent media from the chamber. The scale bars denote 100 microns.

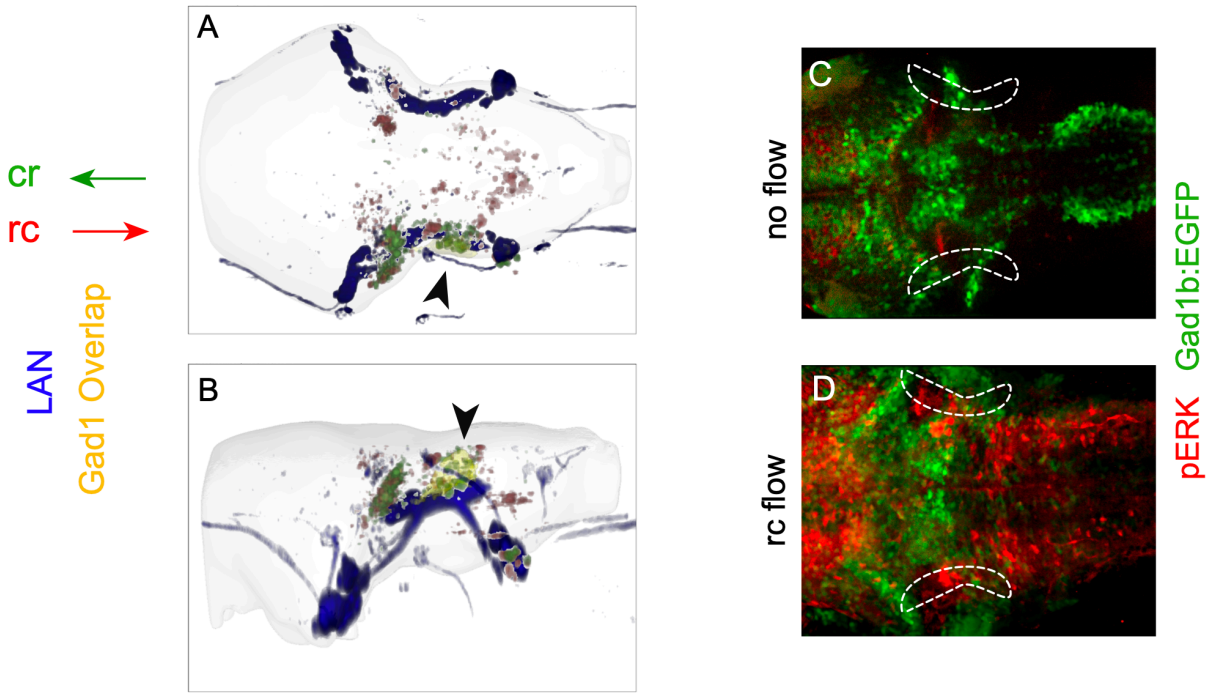

Figure S4. Mapping of neuronal activity in the hindbrain. Related to Figure 4. (**A-B**) Dorsal (A) and lateral (B) views of a three-dimensional-reconstructed reference brain (transparent gray surface). Overlaid Sill:mCherry signal (blue), binary mask of the Gad1b signal (yellow), cr functional map (green), rc functional map (red). Note the overlap between the Gad1b signal and the cr functional map (indicated with a black arrowhead). (**C-D**) Dorsal view or a larval zebrafish expressing Gad1:EGFP (green) and immunostained with an antibody to pERK (red). (C) is a sample subject to no water flow, and (D) is a specimen maintained under continuous laminar water flow for 2 minutes. The white dotted areas indicate the location of the lateralis central lintel in the hindbrain (central arbors).

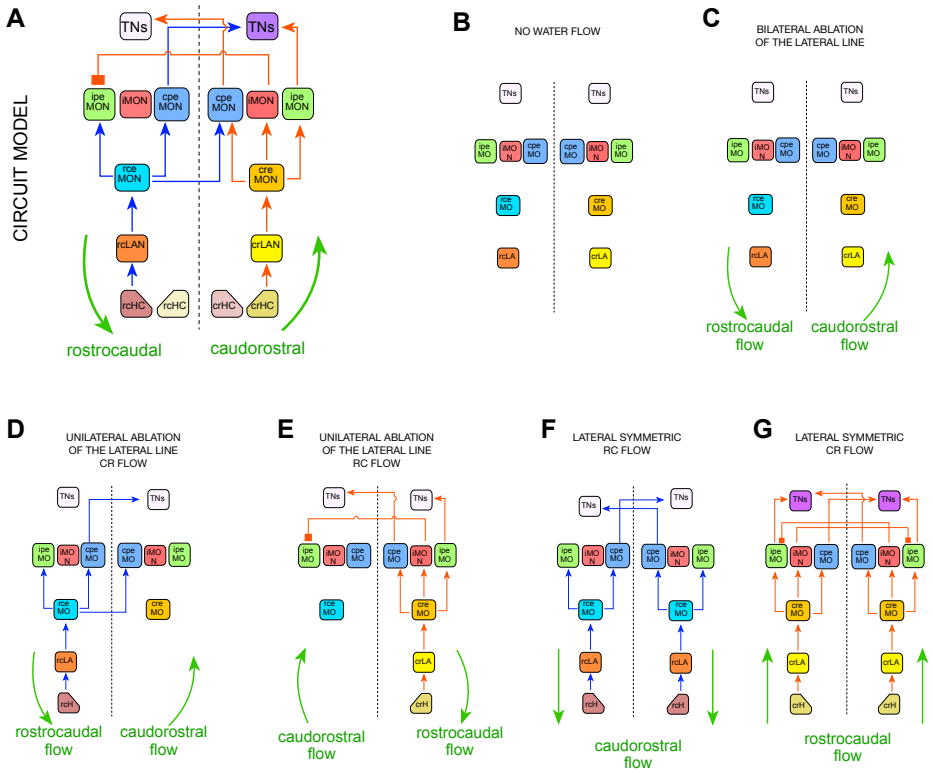

Figure S5. Assessment of the circuit model. Related to Figure 5. (**A**) Proposed circuit model. (**B**) The trivial situation in which under now flow, lack of stimulation of hair cells produces no sensory signal transmission and no activity in toral neurons (TNs) (lilac). (**C**) Identical outcome results from elimination of the lateral line in the presence of water flow. In this case, rheotaxis is disrupted. (**D-E**) Oteíza and colleagues have shown that when one side of the lateral line is eliminated, rheotaxis is severely impaired, indicating that +/∅ does not provide enough information, and that the fish needs +/- to determine flow direction. We have confirmed this result. The model circuit explains this result because if one side of the PLL is eliminated, directional information is persistently asymmetric, eliminating the capacity of the brain to use local rotational flow to determine flow direction. The model circuit captures the outcome regardless of the handedness of the local vortex: counter-clockwise in D and clockwise in E. (**F-G**) If the flow is lateral symmetric, no gradient across the horizontal plane develops, and the animals experiences no rotational flow around its body. In this case, the fish can detect the presence of flow, but it cannot determine its direction because it will experience no differences in flow regime after each swim bout. The model circuit also captures this feature because in cases of lateral symmetric rostrocaudal (F) or caudorsotral (G) flow, symmetry

cannot be broken and information transmission to the brain is vectorially ambiguous.